

Synthesis of Prussian Blue and Its Electrochemical Detection of Hydrogen Peroxide Based on Cetyltrimethylammonium Bromide (CTAB) Modified Glassy Carbon Electrode

A. M. Farah¹, C. Billing², C. W. Dikio¹, A. N. Dibofori-Orji³, O. O. Oyedeji⁴, D. Wankasi¹,
F. M. Mtunzi¹, E. D. Dikio^{1,*}

¹Applied Chemistry and Nanoscience Laboratory, Department of Chemistry, Vaal University of Technology, P. O. Box X021, Vanderbijlpark 1900, Republic of South Africa.

²School of Chemistry, University of the Witwatersrand, P.O Box 3 WITS 2050, Johannesburg, Republic of South Africa

³Department of Chemistry, Ignatius Ajuru University of Education, Rumuolumeni, Port Harcourt, Nigeria

⁴Department of Chemistry, University of Fort Hare, Private Bag X1314, Alice 5700, South Africa

*E-mail: ezekiield@vut.ac.za.

Received: 24 July 2013 / Accepted: 30 August 2013 / Published: 25 September 2013

This paper reports on the modification of glassy carbon electrode with both Prussian blue (PB) and cetyltrimethylammonium bromide (CTAB) for the detection of hydrogen peroxide in acidic and neutral media. Prussian blue was synthesized and characterized by Fourier transform infrared spectroscopy (FT-IR), Ultraviolet-visible spectroscopy (UV-vis), Thermogravimetric analysis (TGA) and Energy dispersive spectroscopy (EDS). The electrochemical behavior of the GC, GC-PB, GC-CTAB and GC-CTAB-PB electrodes were studied by cyclic and square wave voltammetry in acidic and neutral media for the detection of hydrogen peroxide. The result indicates that the modification of the glass carbon (GC) electrode with Prussian blue and cetyltrimethylammonium bromide, a cationic surfactant, promotes cathodic and anodic redox reactions. The cathodic current observed is due to a one electron reduction of Prussian blue.

Keywords: Hydrogen peroxide, Cetyltrimethylammonium bromide, Prussian blue, Glassy Carbon Electrode

1. INTRODUCTION

Prussian blue (PB) is a polynuclear and mixed-valent iron cyanide complex with a repeating unit of potassium ferrous ferricyanide hexacyano hexahydrate $\text{Fe}_4^{111}[\text{Fe}^{\text{II}}(\text{CN})_6]_3$ and well known as an artificial per-oxidase [1-3]. However Prussian blue and its analogues have unique properties such as

electrochromic, electrochemical, photophysical, magnetic and properties among others [4-6]. These unique properties of PB have been broadly used for construction of biosensor because of its peculiar structure and have a perfect catalytic activity towards the reduction of hydrogen peroxide [7-8]. Solid Prussian blue nanoparticles can be synthesized by the addition of an aqueous solution of iron(III) ions to an aqueous ferrocyanide solution under vigorous stirring at room temperature [9-10]. Among inorganic materials that has been used to immobilize the electrode surface with the ability to detect hydrogen peroxide in solution is PB, but its detection ability diminishes in neutral solutions. However, it has been reported that problems caused by leakage of PB layer in solution phase after a few scans at neutral pH is due to the relatively weak combination between PB and the bare electrode [11-13]. So to efficiently enhance the electrochemical stability of PB film, screen-printed electrodes (SPEs) [14], ordered mesoporous carbon (OMC) [15], polyaniline (PANI), multi-walled carbon nanotubes (MWCNTs) [16], graphene oxide (GO) [17-18] and cetyltrimethylammonium bromide (CTAB) [19] have been used to immobilize PB. Surfactants have been used generally to improve the transfer of charges between an electrode and its electroactive specie [20] aimed at facilitating charge transfer between the analyte and the electrode. Cetyltrimethylammonium bromide (CTAB) is cationic surfactant which significantly enhances the rapid transfer of charges [20-21].

Hydrogen peroxide (H_2O_2) is an important analyte, it is an essential byproduct from many peroxidase catalyzed reactions and an important mediator in food, industrial, clinical diagnosis, pharmaceutical and environmental assays [21-22]. Although accurate determination of hydrogen peroxide (H_2O_2) is of considerable interest due to its application. At present, there are several techniques to detect H_2O_2 , which include tetrametry [23], fluorescence [24], chemiluminescence [25] spectrophotometry and electrochemical sensors [26-27]. Among these, electrochemical sensors are the best method due to their intrinsic simplicity, high sensitivity and selectivity [28]. In this work a glassy carbon electrode (GCE) modified with Prussian blue and cetyltrimethylammonium bromide (CTAB) films was developed to determine hydrogen peroxide in acidic as well as in neutral media.

2. EXPERIMENTAL

2.1. Reagents and apparatus

Glassy carbon electrodes (GCE) were purchased from BAS Inc (Tokyo Japan), Sodium dihydrogen phosphate (NaH_2PO_4), disodium hydrogen phosphate (Na_2HPO_4), cetyltrimethylammonium bromide (CTAB), potassium hexacyanoferrate ($\text{K}_4[\text{Fe}(\text{CN})_6]3\text{H}_2\text{O}$), iron nitrate nanohydrate ($\text{Fe}(\text{NO}_3)_3 \cdot 9\text{H}_2\text{O}$) and alumina oxide (Al_2O_3) as well as acetone ($\text{C}_3\text{H}_6\text{O}$), *N,N*-dimethylformamide (DMF), hydrogen peroxide (H_2O_2), hydrochloric acid (HCl) were purchased from Sigma–Aldrich. All chemicals were of analytical grade and used as received without further purification.

2.2. Electrochemical measurements

Electrochemical measurements were performed using an auto-lab potentiostat (663 VA stand metrohm Swiss made). A convectional three- electrode system was employed Ag/AgCl (3M KCl) as a

reference electrode, platinum electrode as a counter electrode and glassy carbon electrode (GC) modified with cetyltrimethylammonium bromide (CTAB) and Prussian blue (PB) as working electrode for all experiments. A 0.1M phosphate buffer solution (PBS) with different pH solutions was used as an electrolyte solution.

2.3. Synthesis and preparation of modified electrodes

The method of synthesis of Prussian blue nanoparticles has been reported in our previous work [29]. The GCE surfaces (3 mm in diameter) were cleaned by gentle polishing in aqueous slurry of alumina oxide nanopowder (Sigma-Aldrich) on a mesh paper. The electrode was then subjected to ultrasonic vibration in acetone to remove residual alumina particles that might be trapped at the surface of the electrode, and then subjected to ultrasonic vibration in deionized water before drying. GC-CTAB was prepared with 50 mg of CTAB dispersed in 5 ml of *N,N*-dimethylformamide (DMF) with the aid of ultrasonic mixing for 15 min to form homogenous suspension. About 20 μL drop of CTAB/DMF solution were dropped on bare GC electrode and dried in an oven at 50°C for 5 min. The modified electrode is herein designated as GC-CTAB. The PB film was prepared by sequential deposition method as described by Han *et al* [30]. GC-Bare or GC-CTAB electrodes were immersed in $\text{Fe}(\text{NO}_3)_3 \cdot 9\text{H}_2\text{O}$ solution for 30 min, with stirring after which the electrodes were rinsed, dried and then immersed in $\text{K}_4[\text{Fe}(\text{CN})_6] \cdot 3\text{H}_2\text{O}$ solution and stirred for another 30 min, followed by a re-rinsing and a re-drying processes to complete the deposition cycle. The electrode obtained thereafter, were described as GC-CTAB, GC-PB and GC-CTAB-PB respectively.

2.4. Characterization

The morphological features of synthesized Prussian blue nanoparticles were analyzed by FTIR, Uv-vis, EDS and TGA. IR spectra were recorded using Perkin-Elmer Spectrum 400 FT-IR/FT-NIR spectrometer in the range 400 – 4000 cm^{-1} . UV-vis spectra were recorded on a Perkin-Elmer lambda 25 UV-vis spectrometer. The surface morphology and Energy Dispersive Spectroscopy (EDS), measurements were recorded with a JEOL 7500F Field Emission scanning electron microscope. The thermal behavior of the carbon nanotube and the catalyst were investigated by TGA using a Q500 TGA instrument under an air environment. The prepared MWCNT samples were heated in platinum crucibles with oxygen and nitrogen gases at a flow rate of 40 and 60 mL/min respectively. The dynamic measurement was made between ambient and 1000°C with a ramp rate of 10°C/min to 900°C.

3. RESULTS AND DISCUSSION

The Fourier transform infrared spectra of Prussian blue and Prussian blue doped cetyltrimethylammonium bromide (CTAB) is presented in figure 1. The FT-IR spectra of Prussian blue nanoparticles show several peaks, figure 1(a), the strong peak at 2057 cm^{-1} which is the characteristic absorption peak of PB is assigned as the stretching vibration of $\text{C}\equiv\text{N}$ group in potassium

hexaferricyanide. The absorption bands near 3215 and 1602 cm^{-1} is assigned to the O–H stretching mode and H–O–H bending mode respectively, which indicate the existence of interstitial forces of attraction in the sample.

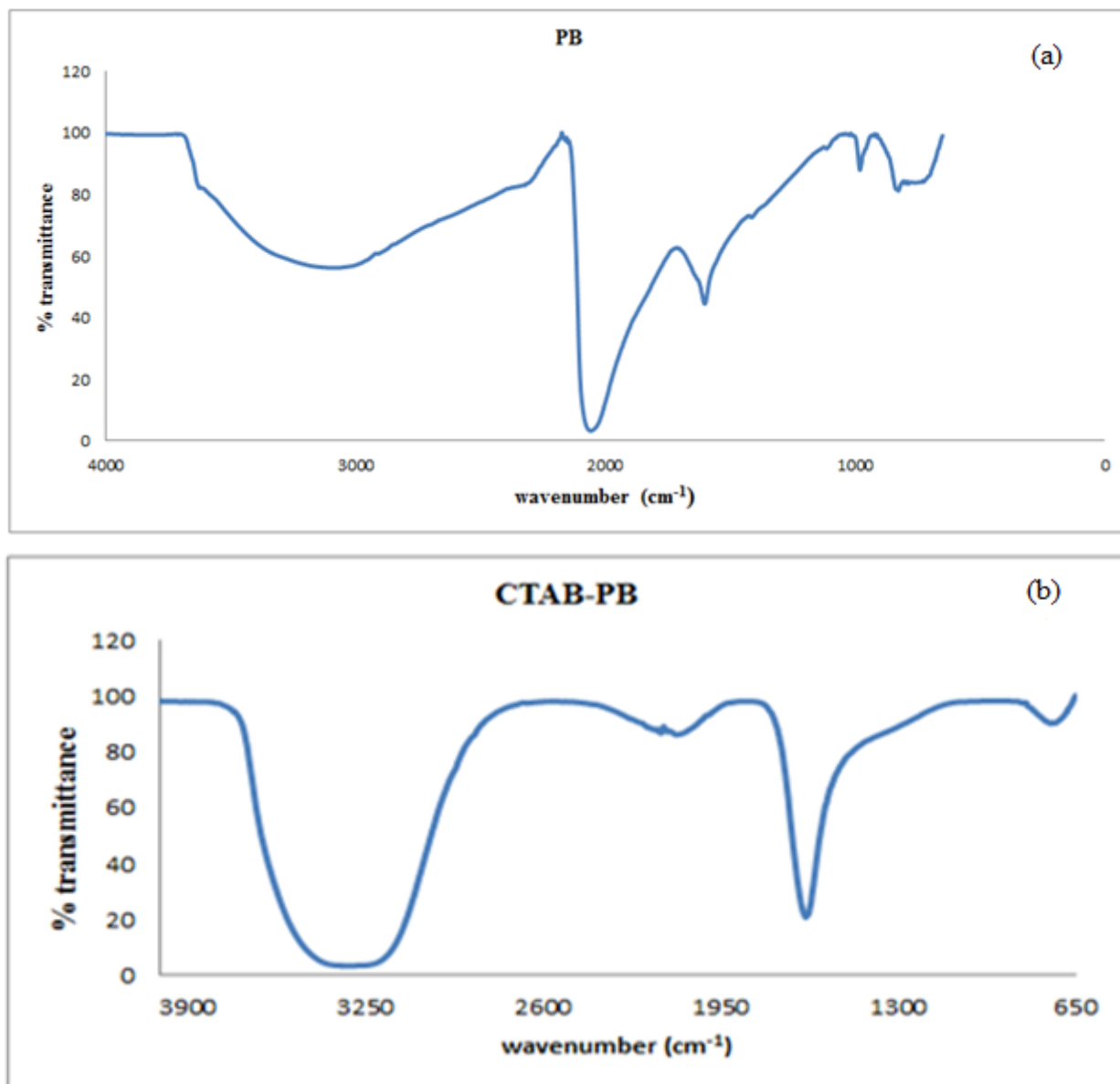


Figure 1. Fourier transform infrared (FT-IR) spectra of (a) Prussian blue (b) Prussian blue-cetyltrimethylammonium bromide nanocomposite.

The absorption bands around 600 cm^{-1} , are due to the structure of $\text{Fe}^{2+}\text{-CN-Fe}^{3+}$ linkage of Prussian blue [4,12,30]. The FT-IR spectra of PB-CTAB nanocomposite, figure 1(b), show new absorption bands formed due to the combination of PB with CTAB. Two important absorption bands are observed in the spectrum demonstrating the interaction between PB and CTAB. The broad band at 3250 cm^{-1} is an O–H stretching mode while the band at 1673 cm^{-1} is a H–O–H bending vibration. The

absorption bands at about 600 cm^{-1} due to iron(II)-CN-iron(III) of Prussian blue disappeared as PB interacted with CTAB.

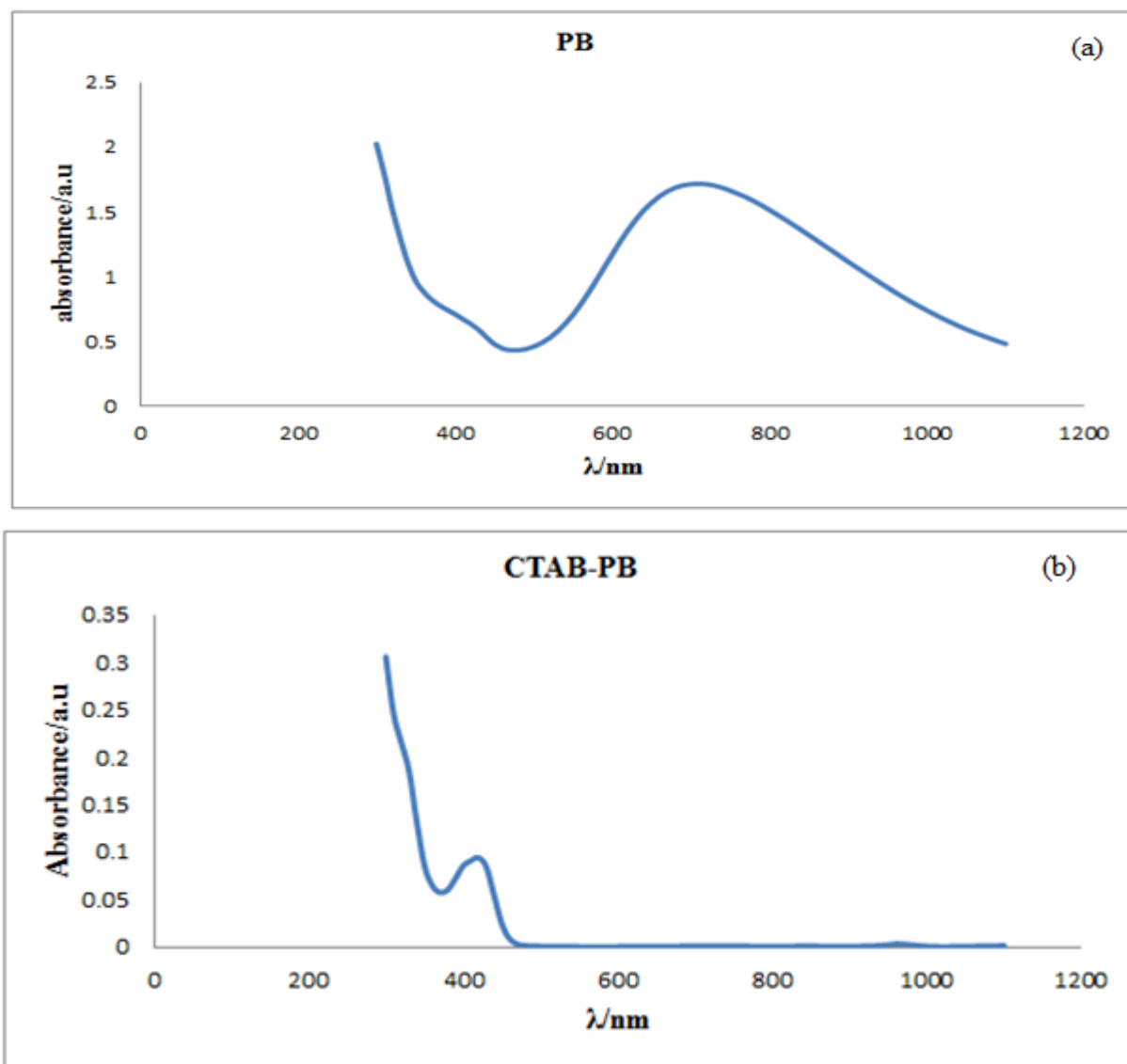


Figure 2. Uv-visible spectra of (a) Prussian blue (b) Prussian blue-cetyltrimethylammonium bromide nanocomposite.

The ultraviolet-visible spectrum of Prussian blue and Prussian blue-Cetyltrimethylammonium bromide composite is presented in figure 2. The spectrum of PB show a broad absorption peak at 700 nm which is the intense charge transfer absorption band due to $\text{Fe}^{2+}\text{-CN-Fe}^{3+}$ polymeric sequence of PB, figure 1(a) [12,31]. The UV-vis spectrum for the nanocomposite, figure 1(b), show an absorption peak at 400 nm, a shift of about 300 nm, which we attribute to be due to the presence of cetyltrimethylammonium bromide ion.

The thermogravimetric analysis (TGA) profile of the Prussian blue is presented in figure 3. TGA analysis was employed to examine the thermal stability of the prepared Prussian blue

nanoparticles. Thermogravimetric analysis (TGA) of weight loss is in most instances used to investigate the presence of nanoparticles in nanomaterials. The interpretations of these curves are not straight forward due to the presence of catalyst particles during weight loss analysis.

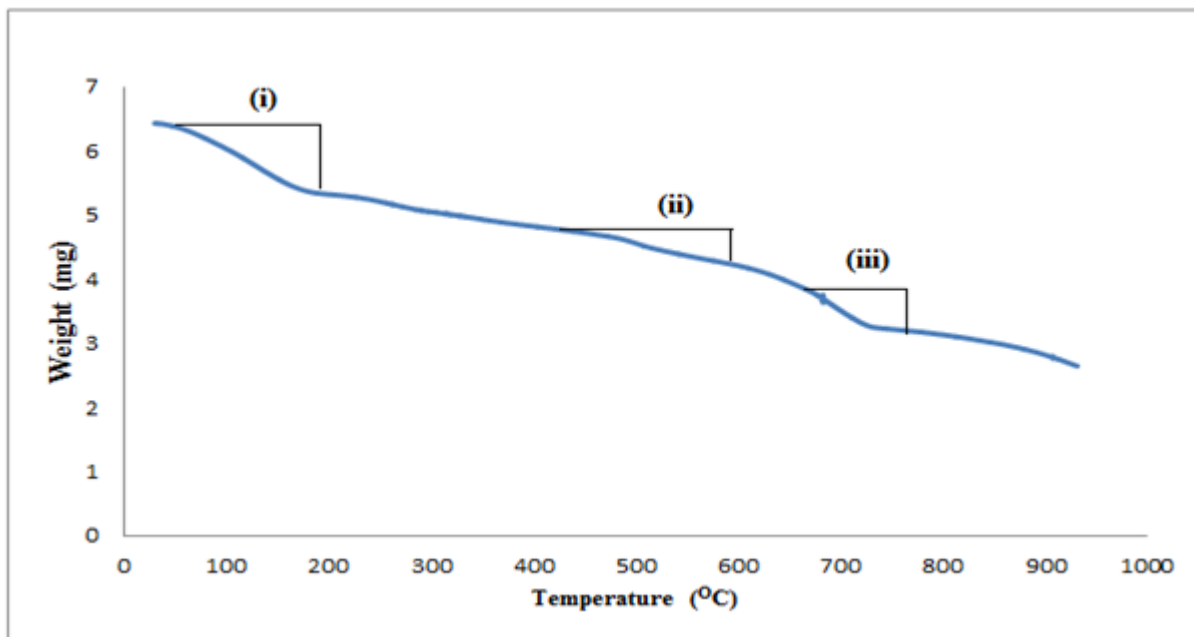


Figure 3. Thermogravimetric analysis (TGA) of Prussian blue nanoparticles.

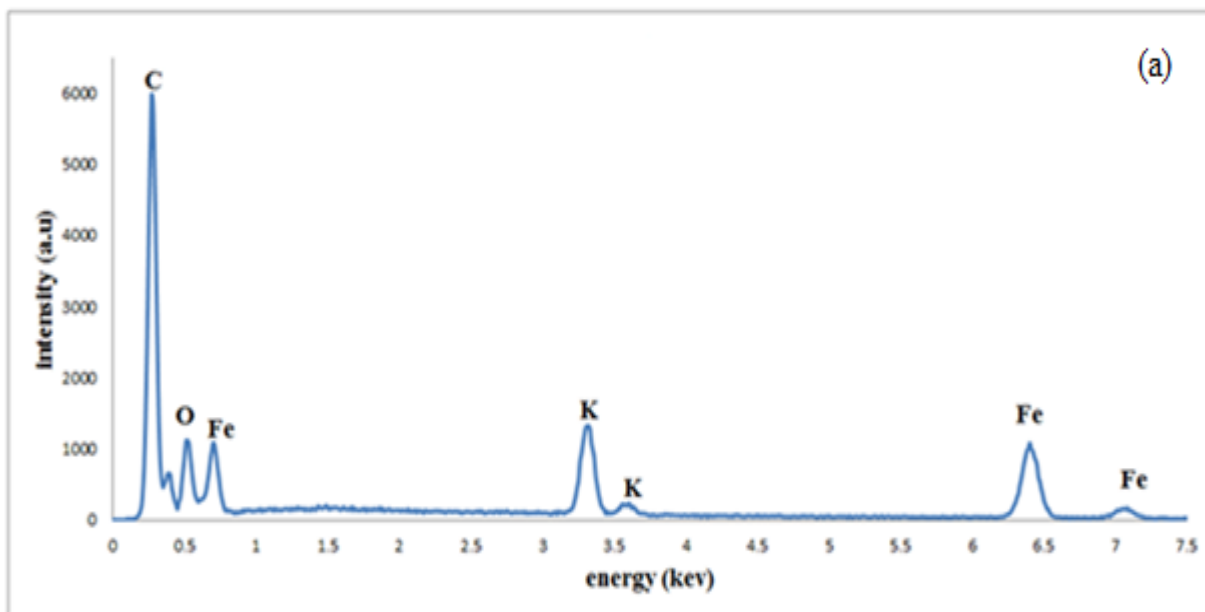


Figure 4. Energy Dispersive spectroscopy (EDS) spectra of Prussian blue nanoparticles.

The temperature at which the Prussian blue nanoparticles oxidized is an index of its stability. The TGA graph show about three weight loss areas in the PB, figure 3(a). Three weight loss regions

labeled (i), (ii) & (iii) are observed in the thermogram. The first weight loss, (i), started at about 100°C and ended at 120°C, this may correspond to the elimination of intrinsically absorbed water molecules in the Prussian blue moiety.

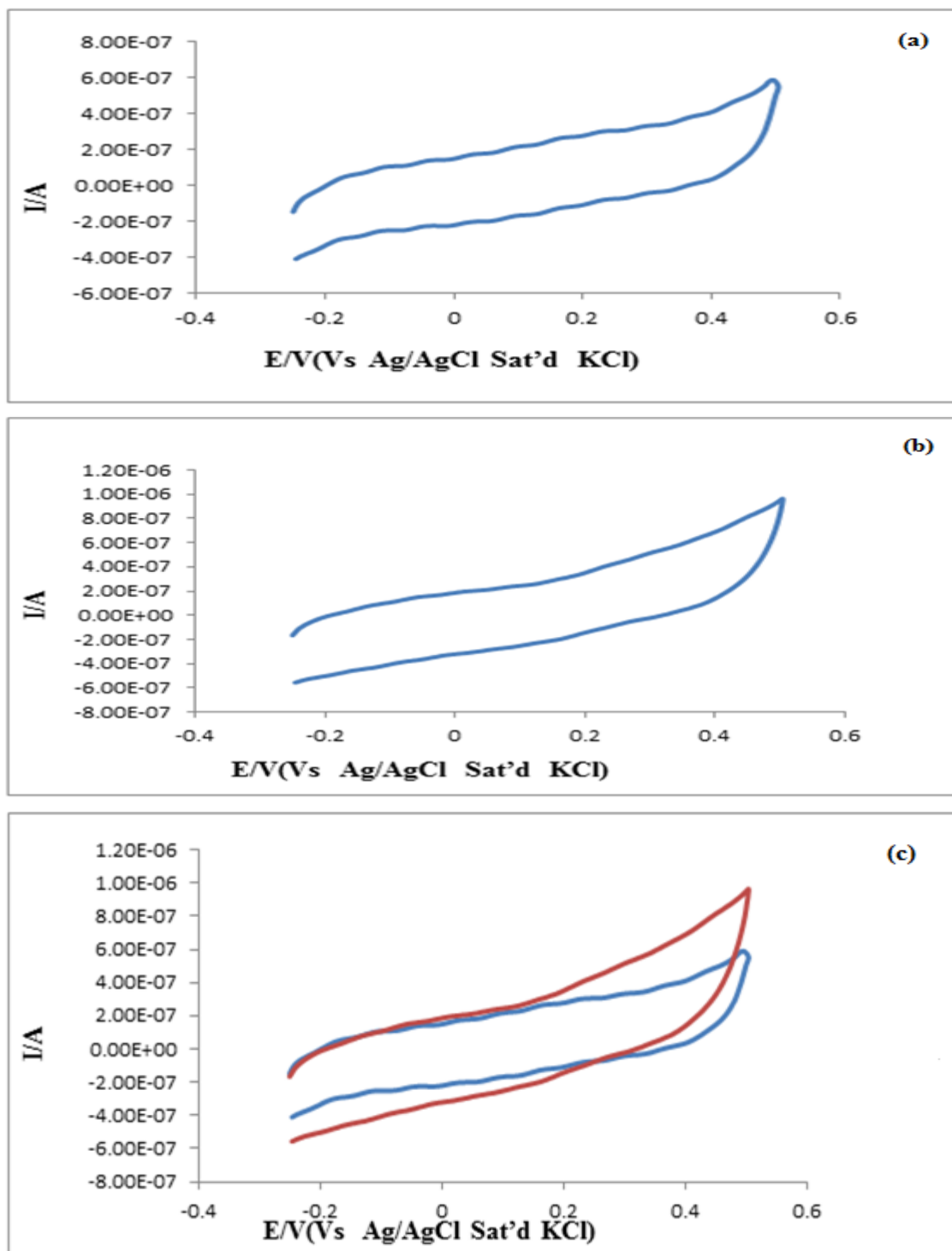


Figure 5. Cyclic voltammograms of bare-GC electrode (a) absence and (b) presence of 25µl H₂O₂ in 0.1M PBS and (c) overlay of the two.

The second and last weight losses at between 450 to 600°C, (ii) and at 680 to 750°C, (iii) are not very large but could be attributed to the presence of soluble and insoluble Prussian blue nanoparticle [23]. Scanning electron microscope [SEM] and X-ray diffraction analysis [XRD] of synthesized Prussian blue nanoparticles used in this study have been reported in a previous publication [4,30]. The energy dispersive spectroscopy (EDS) spectrum of Prussian blue nanoparticle is presented in figure 4. Energy dispersive spectroscopy was employed to identify the presence and absence of element of Prussian blue nanoparticles from our synthesis reaction. The EDS spectra figure 4 show the presence of carbon, oxygen, potassium and iron. Metal elements that constitute Prussian blue in the formula, $\text{Fe}_4[\text{Fe}(\text{CN})_6]_3$ and $\text{KFe}_4\text{Fe}(\text{CN})_6$, the known insoluble and soluble forms of Prussian blue.

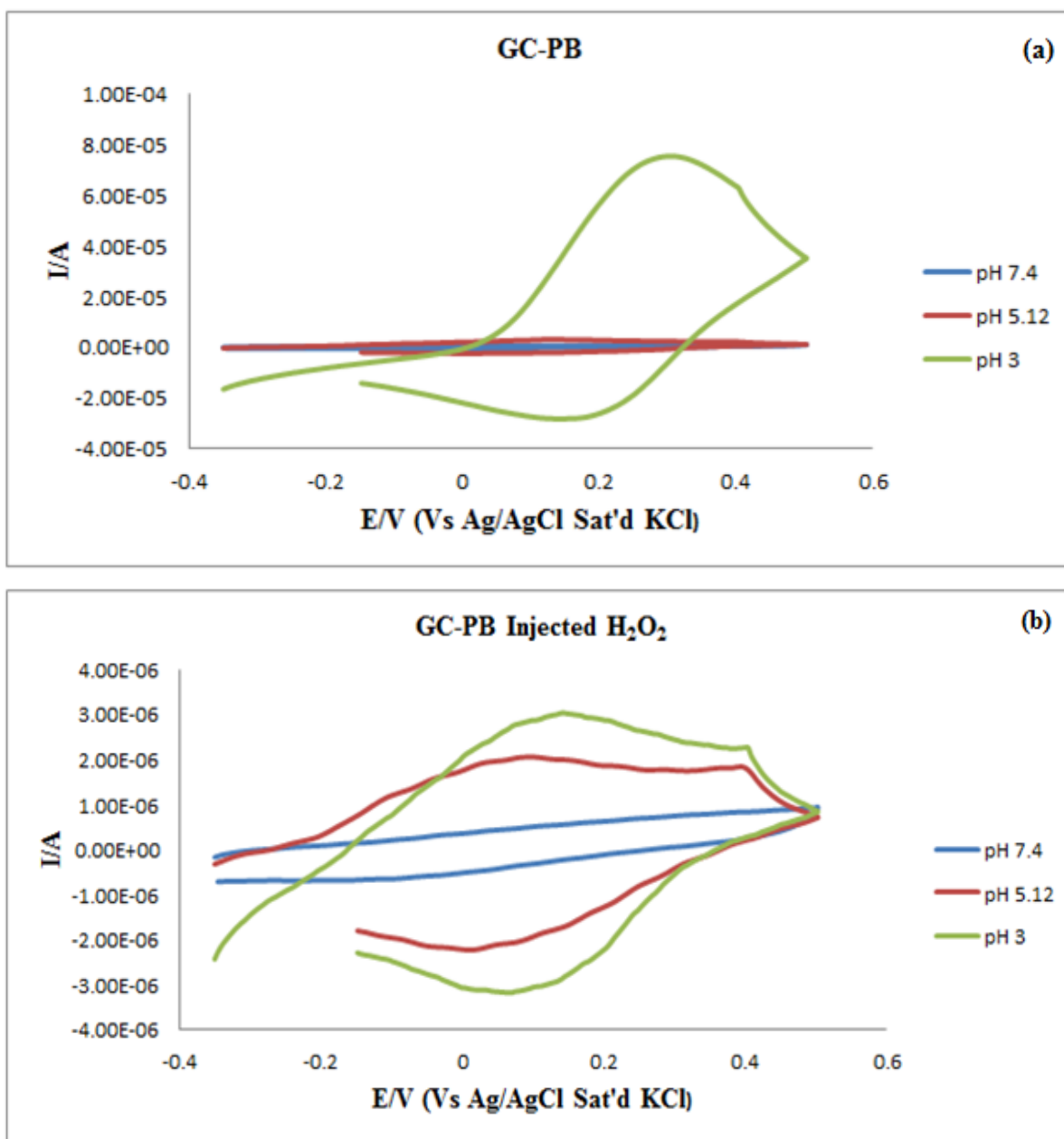


Figure 6. Cyclic voltammograms of GC-PB electrode (a) in the absence and (b) in the presence of 25μl H₂O₂ in 0.1M PBS.

The electrochemical properties of glassy carbon (GC) electrode GC, GC-PB, GC-CTAB, and GC-CTAB-PB electrodes were studied in 0.1 M phosphate buffer solution at different pH values, using cyclic voltammetry recorded between -250 to 500 mV at scan rate of 100 mV/s. The cyclic voltammograms of glassy carbon electrode (GC) in the absence and presence of hydrogen peroxide in 0.1 M phosphate buffer solution at pH 7.4 is presented in figure 5 (a, b & c). The overlay of the electrode response in the absence and presence of hydrogen peroxide is presented in figure 5 (c). As can be seen, a small anodic response is observed as the bare GC electrode does not have the ability to detect hydrogen peroxide.

The cyclic voltammogram of GC-PB electrode in the presence and absence of hydrogen peroxide in 0.1 M phosphate buffer solution at pH 3, pH 5.12 and pH 7.4 are presented in figure 6. The GC-PB electrode in the absence of hydrogen peroxide, figure 6(a) does not show any electrochemical response at pH 5.12 and pH 7.4, while at pH 3, anodic and cathodic responses are observed. In the presence of hydrogen peroxide, figure 6(b), responses are observed at pH 7.4, pH 5.12 and pH 3. The highest response is observed at pH 3 and the lowest response is observed at pH 7.4. The high response at pH 3 is due to the fact that at high pH, Prussian blue loses its stability. Hydrogen peroxide also affects the response of the modified electrode significantly at pH 7.4 and pH 5.12. The cathodic responses are greater than the anodic responses at all pH values. The anodic response at pH 3 for the electrode in the absence of hydrogen peroxide, is also greater than the anodic response in the presence of hydrogen peroxide. On the other hand, the cathodic responses at all pH values in the presence of hydrogen peroxide are greater than the cathodic responses in the absence of hydrogen peroxide.

The cyclic voltammograms of GC-CTAB in the absence and presence of hydrogen peroxide in 0.1 M phosphate buffer solution at pH 7.4 is presented in figure 7 (a, b & c). The overlay of the electrode response in the absence and presence of hydrogen peroxide is presented in figure 7 (c). As can be observed, a small cathodic response is observed by the GC-CTAB electrode in the presence of hydrogen peroxide.

The cyclic voltammograms of GC-CTAB-PB electrode in the absence or presence of hydrogen peroxide in 0.1 M phosphate buffer solution at pH 3, pH 5.12 and pH 7.4 are presented in figure 8. This combination of cetyltrimethylammonium bromide and Prussian blue nanoparticles modified electrode employed to determine the effect of the presence of two substances in the detection of hydrogen peroxide. In the absence of hydrogen peroxide, figure 8(a), anodic responses are observed at all pH values. The highest response is observed at pH 7.4 and the lowest in acidic medium at pH 3. The cathodic response on the other hand is more pronounced at pH 7.4 but less pronounced at pH 5.12 and pH 3. In the presence of hydrogen peroxide, figure 8(b), the GC-CTAB-PB electrode produces both anodic and cathodic responses. One anodic and cathodic peak is observed at pH 7.4 indicating one electron transfer reaction taking place. At pH 5.12, the electrode reaction showed both anodic and cathodic responses with no specific peak in both. Anodic and cathodic responses observed at pH 3 are more pronounced than at pH 5.12. These results indicate the presence of CTAB has considerably enhanced the electrochemical stability of PB film and its detection of hydrogen peroxide. The cyclic voltammograms of GC-PB and GC-CTAB-PB electrode reactions observed could be explained as a one electron transfer reaction in neutral or slightly acidic medium. The cathodic current observed is due to a one electron reduction of Prussian blue, $[\text{Fe}(\text{CN})_6]^{3-} + e^- \rightleftharpoons \text{Fe}(\text{CN})_6^{4-}$. The mechanism of the

redox reaction for soluble PB can be expressed as, $\text{KFe}[\text{Fe}(\text{CN})_6] + \text{K}^+ + \text{e}^- \rightleftharpoons \text{K}_2\text{Fe}[\text{Fe}(\text{CN})_6]$ and for insoluble PB, the mechanism is expressed as: $\text{Fe}[\text{Fe}(\text{CN})_6]_3 + 4\text{K}^+ + \text{e}^- \rightleftharpoons \text{K}_4\text{Fe}_4[\text{Fe}(\text{CN})_6]_3$ [21].

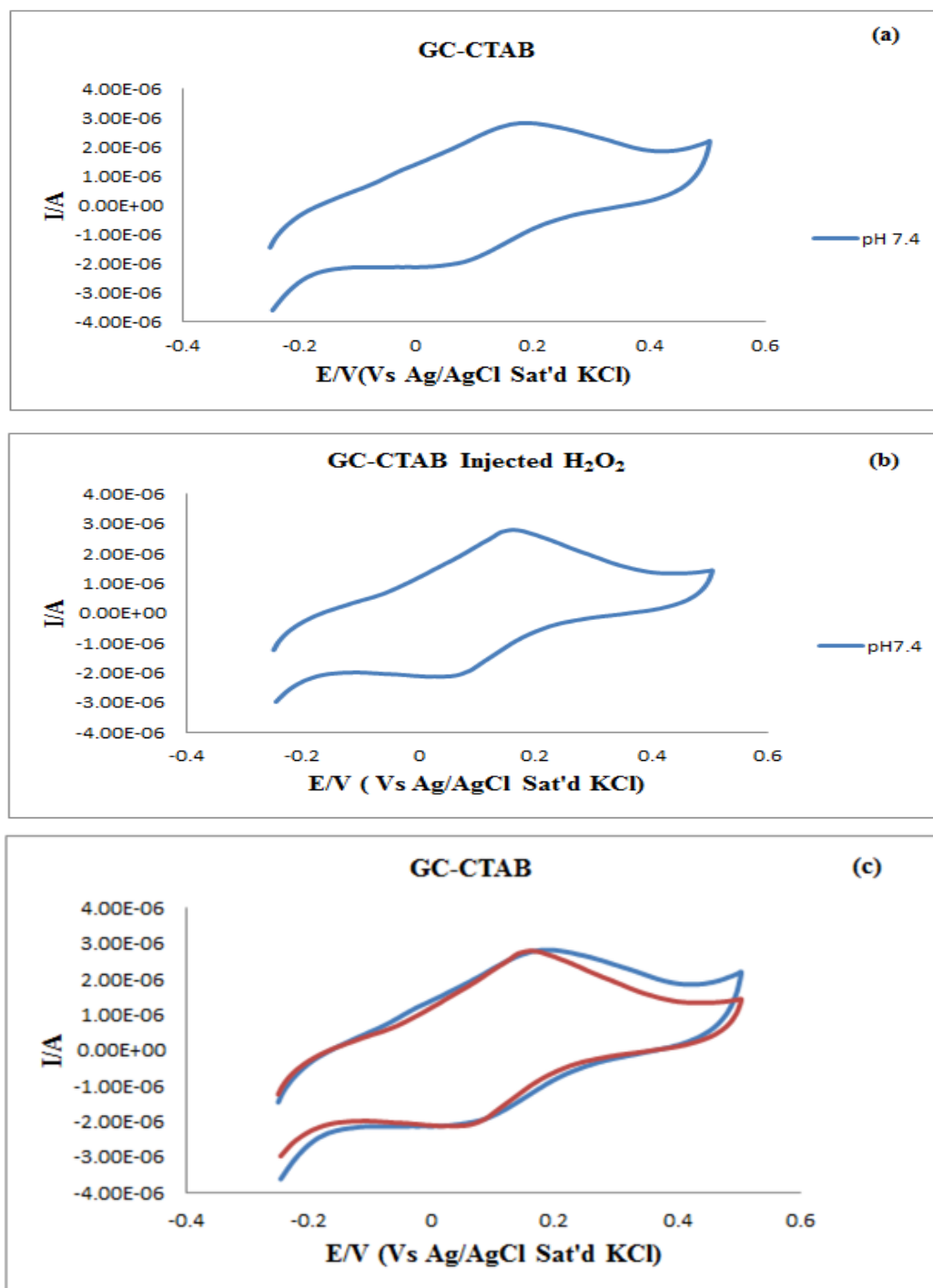


Figure 7. Cyclic voltammograms of GC-CTAB electrode (a) in the absence and (b) in the presence of 25 µl H₂O₂ in 0.1M PBS pH 7.4 and (c) overlay of the two.

The electrochemical properties of GC-CTAB electrode was also studied in 0.1 M phosphate buffer solution at different pH values, using square wave voltammetry recorded between -700 mV to

700 mV at scan rate of 50 mV/s. The square wave voltammograms of glassy carbon electrode modified cetyltrimethylammonium bromide (GC-CTAB) before and after injected of H₂O₂ in 0.1 M phosphate buffer solution at pH 7.4 is presented in figure 9 (a & b).

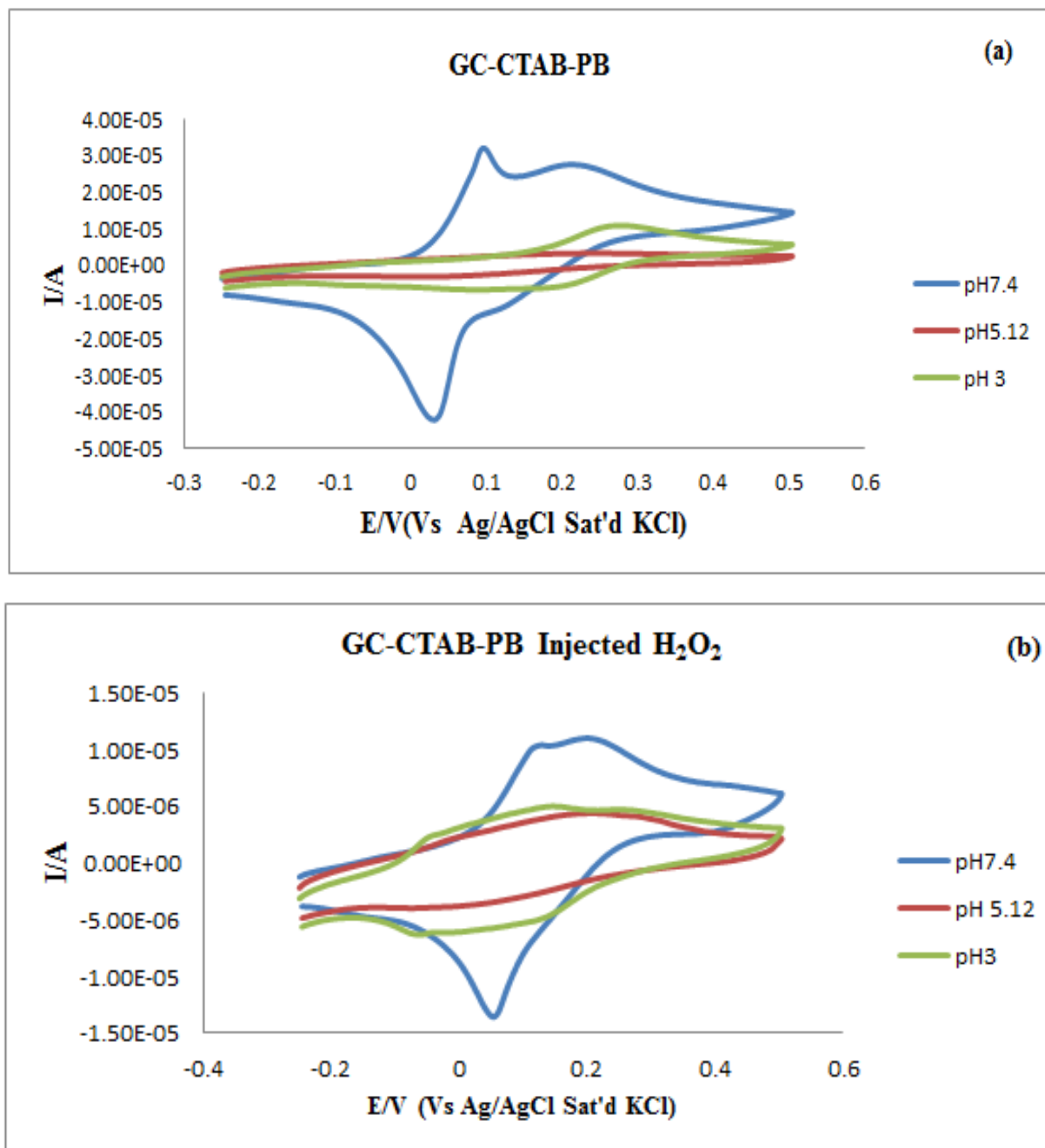


Figure 8. Cyclic voltammograms of GC-CTAB-PB electrode (a) in the absence and (b) in the presence of 25μl H₂O₂ in 0.1M PBS with different pH.

Their overlay is presented in figure 9 (c). These results are in agreement with cyclic voltammogram results presented in figure 5, for GC electrode and for other electrodes in our study [4,30] in which a cathodic current is observed corresponding to a one electron reduction in the presence of hydrogen peroxide is observed.

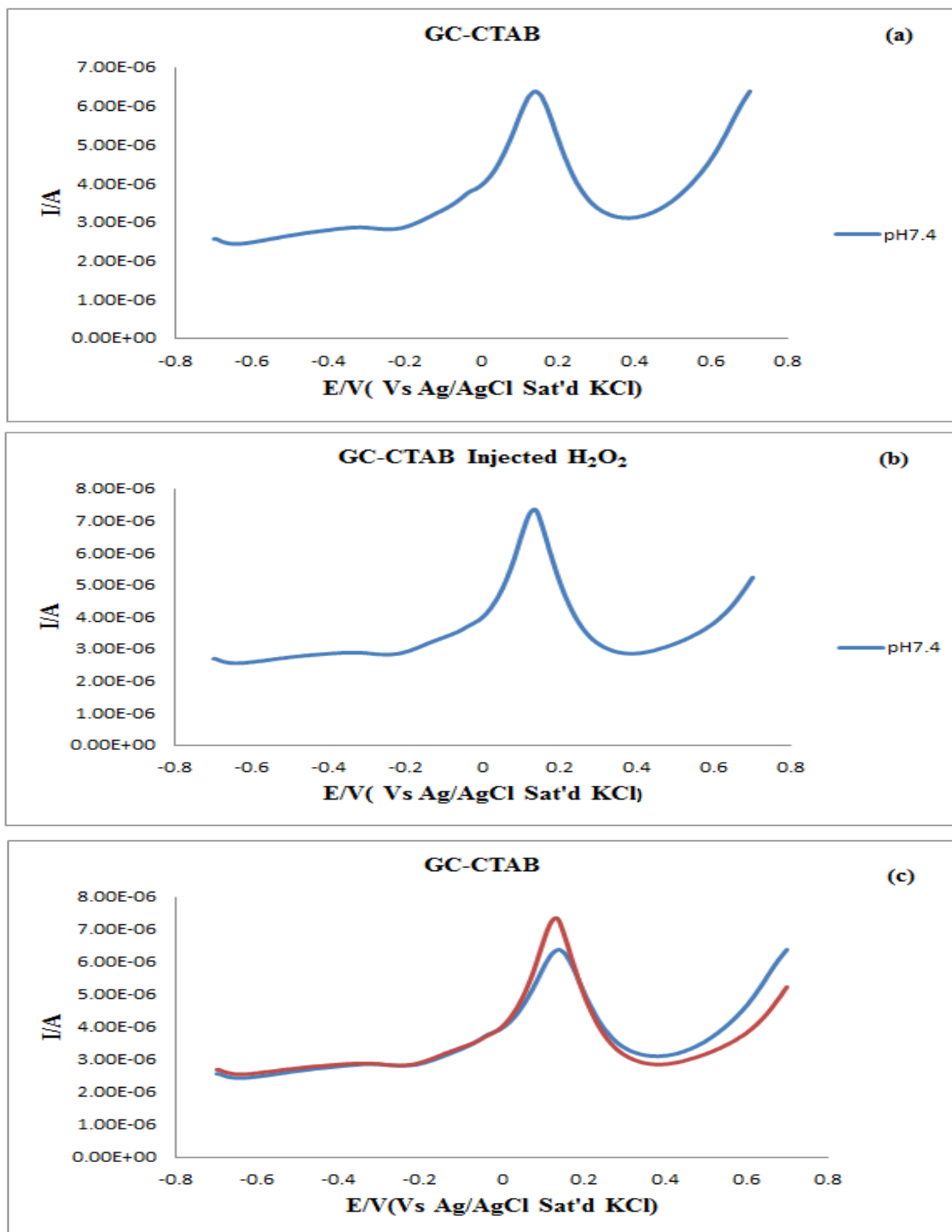


Figure 9. Square wave voltammograms of GC-CTAB electrode (a) in the absence and (b) in the presence of 25 μ l H₂O₂ in 0.1M PBS pH 7.4 and (c) overlay of the two.

Square wave voltammetry of GC-CTAB-PB before and after injection of H₂O₂ in 0.1 M PBS at pH 3, pH 5.12 and pH 7.4 are presented in figure 10 (a & b). In the absence of hydrogen peroxide, figure 10 (a), cathodic current responses are observed. The highest cathodic response is observed at pH 7.4, while at pH 5.12 and 3, lower responses are observed respectively. In the presence of hydrogen

peroxide, figure 10 (b), the GC-CTAB-PB electrode again produced cathodic responses at pH 7.4, 5.12 and 3. The electrode reaction in presence of hydrogen peroxide decrease at pH 5.12, while at pH 7.4 and 3, there were no changes in the electrode response.

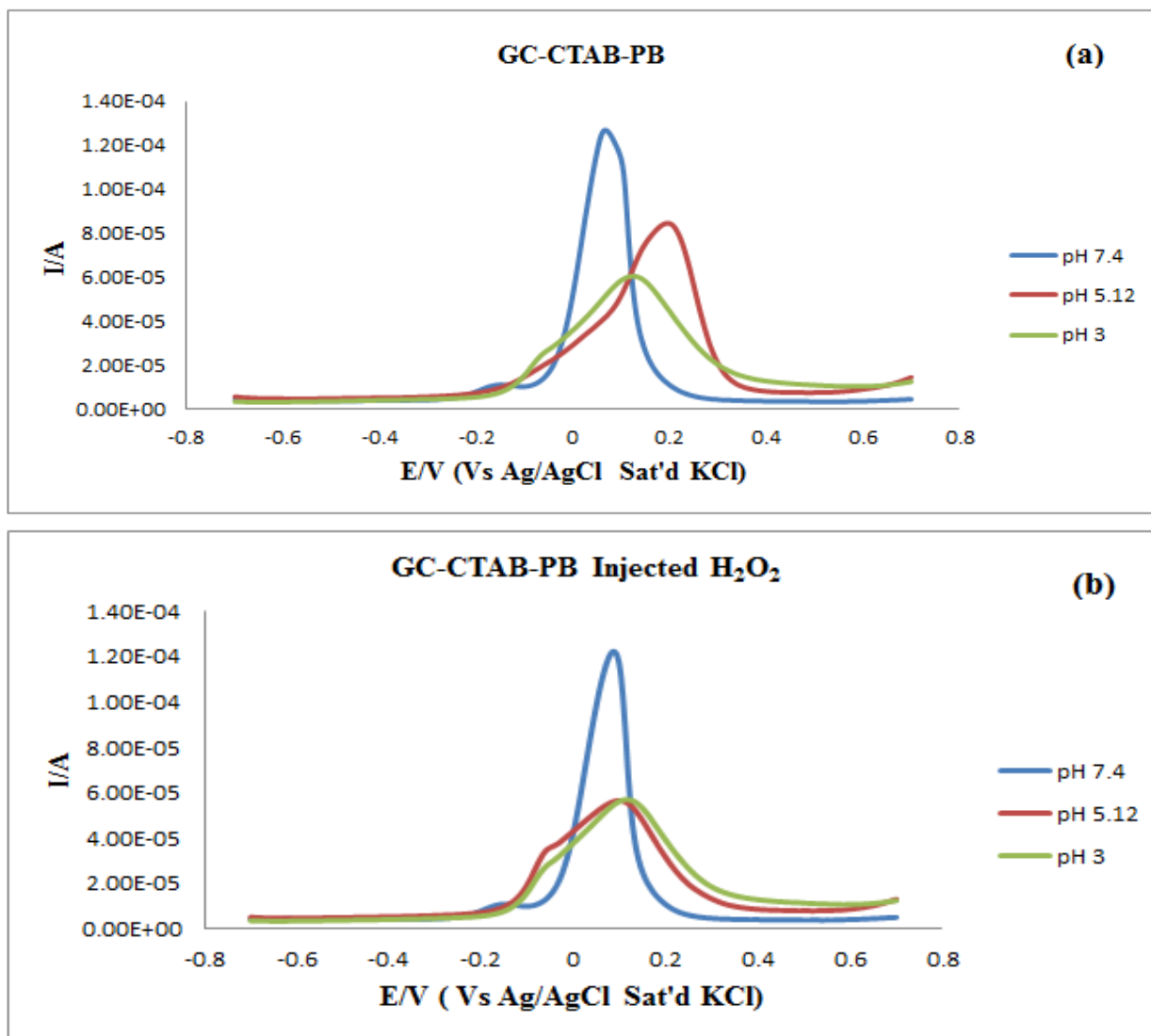


Figure 10. Square wave voltammograms of GC-CTAB-PB electrode (a) in the absence and (b) in the presence of 25 μ l H₂O₂ in 0.1M PBS at different pH values.

The optimum response pH in the square wave voltammetry of GC-CTAB-PB electrode is pH 5.12. This is a slightly acidic medium and confirms cyclic voltammetry result obtained for the same system, figure 8 (b), in which cathodic and anodic responses are observed at pH 5.12 and 3. This implies that the electrochemical property of PB at the electrode surface depends strongly on the pH value of the solution. These results indicates that the modification of the glass carbon (GC) electrode with Prussian blue and cetyltrimethylammonium bromide, a cationic surfactant, promotes cathodic and anodic redox reactions, at the electrode in slightly acidic medium rather than a neutral medium. The presence of CTAB has therefore greatly enhanced the electrochemical stability of PB.

4. CONCLUSION

This study presents the modification of glassy carbon electrode with both Prussian blue and cetyltrimethylammonium bromide for the detection of hydrogen peroxide in acidic and neutral media. Cyclic and square wave voltammetric study of the redox reaction at the modified electrode indicates a one electron transfer reaction in slightly acidic medium.

ACKNOWLEDGMENTS

This work was supported by a research grant from the Research Directorate of the Vaal University of Technology, Vanderbijlpark and the Directorate of Research Govan Mbeki Research and Development Centre, University of Fort Hare.

References

1. A.S. Adekunle, A.M. Farah, J. Pillay, K.I. Ozoemena, B.B. Mamba, B.O. Agboola. *Colloids. Surf. B. Biointerfaces*. 95, 2012, 186-194.
2. B. Haghighi, H. Hamidi, L. Gorton. *Sens. Actuators. B*. 147 (2010) 270-276.
3. Z. Li, J. Chen, W. Li, K. Chen, L. Nie, S. Yao. *J. Electroanal. Chem.* 603 (2007), 59-66.
4. A.M. Farah, .F.T. Thema, E.D. Dikio. *Int. J. Electrochem. Sci.* 7 (2012) 5069-5083
5. L. Cui, J. Zhu, X. Meng, H. Yin, X. Pan, S. Ai, *Sens. Actuators. B*. 161 (2012) 641-647.
6. J. Zhang, J. Li, F. Yang, B. Zhang, X. Yang. *Sens. Actuators. B*143 (2009) 373-380.
7. J. Zeng, W. Wei, X. Liu, Y. Wang, G. Luo. *Microchim. Acta*. 160 (2008) 261-267.
8. J. Tao, G. Xu, H. Hao, F. Yang, K. Ahn, W. Lee. *J. Electroanal. Chem.* 689 (2013) 96-102.
9. M. Shokouhimehr, E.S Soehnlén, A. Khitrin, S. Basu, S.D Huang. *Inorg. Chem. Commun.* 13 (2010) 58-61
10. A. Gotoh, H. Uchida, M. Ishizaki, T. Satoh, S. Kage, S. Okamoto, M. Ohta, M. Sakamoto, T. Kawamoto, H. Tanaka, M. Tokumoto, S. Hara, H. Shiozaki, M. Yamada, M. Miyake, M. Kurihara. *Nanotech.* 18 (2007) 345609 (6pp).
11. C. Wang, L. Zhang, Z. Guo, J. Xu, H. Wang, H. Shi, K. Zhai, X. Zhuo. *Electroanalysis*. 22(16) (2010) 1867-1872.
12. L. Lin, X. Huang, L. Wang, A. Tang. *Solid. State. Sci.* 12 (2010) 1764-1769.
13. S. Liu, H. Li, W. Sun, X. Wang, Z. Chen, J. Xu, H. Ju, H. Chen. *Electrochem. Acta*. 56 (2011) 4007-4014.
14. F. Ricci, A. Amine, G. Palleschi, D. Moscone. *J. Biosens. Bioelectron.* 18 (2003) 165-174.
15. J. Bai, B. Qi, J.C. Ndamaniha, L.P. Guo. *Micropor. Mesopor. Mater.* 119 (2009) 193-199.
16. N. Zhang, G. Wang, A. Gu, Y. Feng, B. Fang. *Mirochim. Acta*. 168 (2010) 129-134.
17. E. Jin, X. Lu, L. Cui, D. Chao, C. Wang. *Electrochem. Acta*. 55 (2010) 7130-7234.
18. Y. Zhang, X. Sun, L. Zhu, H. Shen, N. Jia. *Electrochim. Acta*. 56 (2011) 1239-1245.
19. R. Vittal, K.J. Kim, H. Gomathi, V. Yegnaraman. *J. Phys. Chem. B* 112 (2008) 1149-1156.
20. P. Salazar, M. Martin, R.D. O'Neill, R. Roche, J.L Gonzalez-Mora. *Colloids. Surf. B. Biointerfaces*. 92 (2012) 180 – 189.
21. D-J. Yang, C-Y. Hsu, C-L. Lin, P-Y. Chen, C-W. Hu, R. Vital, K-C. Ho. *Sol. Energy. Mater. Sol. Cells*. 99 (2012) 129-134.
22. J. Yang, N. Myoung, H. Hong. *Electrochim. Acta*. 81 (2012) 37-43.
23. Y. Miao, J. Chen, X. Wu, J. Miao. *Colloids Surf. A.: Physicochem. Eng. Asp.* 295 (2007) 135 – 138.
24. N.V. Klassen, D. Marchington, H.C.E. McGowan. *Anal. Chem.* 66 (1994) 2921-2925.

25. M. Abo, Y. Urano, K. Hanaoka, T. Teria, T. Komatsi, T. Nagano. *J. Am. Chem. Soc.* 133 (2011) 10629-10637.
26. B. X. Li, Z. J. Zhang, Y. Jin. *Sens. Actuators. B.* 72 (2001) 115-119.
27. H. Lu, S. Yu, Y. Fan, C. Yang, D. Xu. *Colloids. Surf. B. Biointerfaces.* 101 (2013) 106-110.
28. S. Woo, Y.R. Kim, T.D. Chung, Y. Piano, H. Kim. *Electrochim. Acta.* 59 (2012) 509-514.
29. Y. Zhang, Y. Liu, J. He, P. Pang, Y. Gao, Q. Hu. *Electrochim. Acta.* 90 (2013) 550-555.
30. A.M. Farah, N.D. Shooto, F.T Thema, J. S Modise, E.D. Dikio. *Int. J. Electrochem. Sci.* 7 (2012) 4302-4313.
31. Y. Zhang, Y. Wen, Y. Liu, D. Li, J. Li. *Electrochem. Commun.* 6 (2004) 1180 – 1184.